




# Atomic-scale understanding of interstitial-strengthened high-entropy alloys

Qiang Yu, Shi Qiu, Zeng-Bao Jiao\* 

Received: 31 October 2024 / Revised: 14 March 2025 / Accepted: 16 March 2025 / Published online: 23 May 2025  
© The Author(s) 2025

**Abstract** Interstitial alloying has emerged as a powerful strategy to tune microstructure and microproperties of high-entropy alloys (HEAs) due to the strong interaction of interstitials with constituent elements and crystal defects, which enables the development of advanced alloys with superior mechanical and functional properties. The paper reviews the latest progress in the atomic-scale understanding of the effects of various interstitials, including carbon, boron, nitrogen, oxygen, and hydrogen, on the microstructure, stability, mechanical properties, and deformation behavior of HEAs. Emphases are placed on the in-depth insights on the interaction of interstitials with constituent elements and crystal defects, such as vacancies, stacking faults, and grain boundaries. Key parameters for rapid prediction of intrinsic properties of HEAs are also discussed. Finally, we highlight some unsolved issues and provide perspectives for future research directions.

**Keywords** High-entropy alloy; Interstitial; Atomistic modeling; Mechanical property; Deformation mechanism

## 1 Introduction

High-entropy alloys (HEAs), comprising multiple principal elements in equal or nearly equal concentrations, have

received enormous attention due to their unique microstructure and attractive properties [1, 2]. Originated from the “high entropy” concept, conventional HEAs primarily form substitutional solid solutions with a face-centered cubic (FCC), body-centered cubic (BCC), or hexagonal-closed packed (HCP) structure. The size and modulus mismatch among constituent elements contribute to a pronounced lattice distortion and substantial solid solution strengthening. Such a unique strengthening effect is considered to be the main cause of exceptional mechanical properties of HEAs, and various models and theories have been developed to describe the solid solution strengthening in HEAs. Recently, interstitial alloying is found to be very attractive in providing remarkable solid solution strengthening due to the large distortion induced by small-sized interstitials [3, 4]. Over the past decade, this strategy has been widely used in HEAs and provides tremendous opportunities in improving mechanical properties of HEAs [5].

Generally, interstitials can either segregate to grain boundaries (GBs) or reside in grain interiors in crystalline metallic materials. For the former, carbon, boron, and nitrogen usually form a predominantly covalent bond with the d-band of their neighboring metals, which increases the GB cohesion. By contrast, oxygen and hydrogen usually produce negative charged ions, which decreases the GB cohesion and promotes the intergranular embrittlement [6]. For the latter, carbon and nitrogen are found to provide a strong solid solution strengthening effect and sometimes induce transformation-induced plasticity (TRIP) and/or twinning-induced plasticity (TWIP) effects [7]. By carefully tailoring the metastability, interstitial-containing solid solution alloys can achieve a good combination of high strength and ductility. In addition to the solid solution

---

Q. Yu, S. Qiu, Z.-B. Jiao\*  
Department of Mechanical Engineering, Research Institute for  
Advanced Manufacturing, The Hong Kong Polytechnic  
University, Hong Kong 999077, China  
e-mail: zb.jiao@polyu.edu.hk

Q. Yu, S. Qiu, Z.-B. Jiao  
The Hong Kong Polytechnic University Shenzhen Research  
Institute, Shenzhen 518057, China



strengthening effect, interstitials in HEAs can induce some unique structural features and novel properties. For example, oxygen and hydrogen are typically considered as harmful elements in conventional metallic materials, which can deteriorate the alloy ductility and toughness. In contrast, hydrogen was reported to suppress the embrittlement and improve mechanical properties of FeCoNiCrMn [8]. Oxygen was found to enhance both strength and ductility of refractory HEAs via forming ordered interstitial complexes (OICs) in chemical short-range order (CSRO) regions [9]. Moreover, some interstitials exhibit high flexibilities in tailoring structures and properties of HEAs. For instance, carbon can trigger either unidirectional [10] or bidirectional [11] FCC-to-HCP phase transformation in Fe<sub>49.5</sub>Mn<sub>30</sub>Co<sub>10</sub>Cr<sub>10</sub>. These interesting observations indicate high potential to design high-performance HEAs through interstitial alloying.

Understanding the underlying mechanisms behind the interstitial alloying and establishing a holistic framework of interstitial effects are crucial for further improving properties of HEAs. However, the mechanisms of the interstitial effects in HEAs are often complicated due to the complex atomic interactions. Computational models and simulations provide powerful tools for interpreting experimental observations from atomic-level insights and guiding materials design with reduced “trial-error” costs. Specifically, through simulating the interactions and arrangements of atoms, these tools provide detailed information on how interstitial alloying influences material behavior at the fundamental level. These atomistic insights are crucial for unraveling how interstitial additions alter the microstructure and properties of materials, thereby providing foundational knowledge and guidelines for the design of advanced materials with desired properties. Motivated by the recent advancement in modeling and simulation of interstitial-strengthened HEAs, this paper aims at providing an overview of the role of interstitials in the microstructure, phase stability, mechanical properties, and deformation behavior of HEAs through computational modeling and simulations. These methods examine the interstitial effects at an atomic level, offering valuable atomic and electronic insights that deepen our understanding of the intrinsic properties of interstitial-strengthened HEAs. The influences of various interstitials, such as carbon, boron, nitrogen, oxygen, and hydrogen, on the intrinsic properties (including solubility, local lattice distortion, and defects energies) of HEAs are systematically analyzed and discussed. Special attention is placed on the in-depth insights on the atomic interactions of interstitials with constituent elements and crystalline defects, such as vacancies, stacking faults (SFs), and GBs (Fig. 1). Finally, we discuss some fundamental and technological areas that should be further explored in future studies.

## 2 Solubility of interstitials in HEAs

Unlike traditional metals and alloys that generally have a low solubility for interstitial atoms, HEAs can provide a substantially high solubility for them, particularly in refractory BCC HEAs. One of the major reasons for the enhanced solubility in HEAs is ascribed to the highly distorted lattice in these materials, which provides numerous interstitial sites. For FCC, BCC, and HCP crystals, the interstitial sites can be divided into two categories, namely octahedral and tetrahedral ones, as shown in Fig. 1. The solubility of interstitials in HEAs can be estimated from the solution energy,  $E_{\text{solution}}$ , which can be obtained by

$$E_{\text{solution}} = E_{(\text{HEA} + \text{interstitial})} - (E_{\text{HEA}} + E_{\text{interstitial}}) \quad (1)$$

where  $E_{(\text{HEA} + \text{interstitial})}$  and  $E_{\text{HEA}}$  are the energies of the HEA per formula unit with and without one interstitial atom, respectively, and  $E_{\text{interstitial}}$  is the energy of the interstitial atom in its stable state.

Through density functional theory (DFT) calculations, it is found that hydrogen, carbon, nitrogen, and boron all prefer to occupy the octahedral sites in FCC HEAs [12–16]. Specifically, the order of the average formation energies for interstitials in FeCoNiCr is C (0.74 eV) > N (0.36 eV) > H (0.13 eV) [17], as displayed in Fig. 2A. It was found that the behavior of interstitial atoms in a solution is closely related to their local atomic configurations. For example, nitrogen exhibits low dissolution energies at sites with more chromium atoms, whereas carbon shows low dissolution energies at sites with fewer nickel atoms. This suggests a strong attraction between chromium and nitrogen and a significant repulsive interaction between carbon and nickel [16, 17]. Song et al. [16] examined the formation energy of doping carbon, boron, and silicon into FeCoNiCr to assess the phase stability of the materials (Fig. 2B). They found that Si-doped FeCoNiCr HEAs have significantly higher average formation energies compared to C- and B-doped HEAs, indicating that Si-doped FeCoNiCr HEAs are relatively more challenging to synthesize. The instability of Si-doped FeCoNiCr HEAs can be ascribed to the severe lattice distortion induced by the larger atomic radius of Si atoms [16]. Zhou et al. [18] found that HEAs with low hydrogen diffusion coefficients typically have high Co and Mn contents, whereas those with high hydrogen diffusion coefficients are rich in Fe and Ni. For refractory BCC HEAs, the probability of site occupancy for oxygen and nitrogen in the octahedral and tetrahedral sites is comparable (Fig. 2C) [9, 19, 20], whereas carbon prefers to occupy the octahedral sites [21].

It has been proposed that the highly fluctuated local chemical environment and the distorted lattice of HEAs

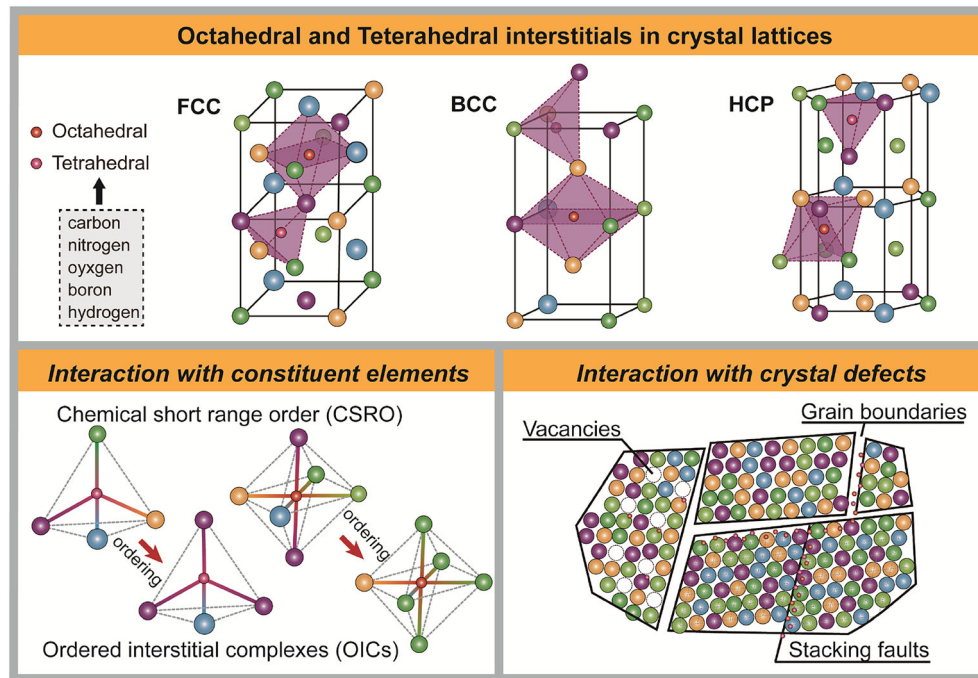


**Fig. 1** Schematic illustration of the available interstitial sites in crystal lattices and interactions of interstitials with constituent elements and crystal defects in HEAs

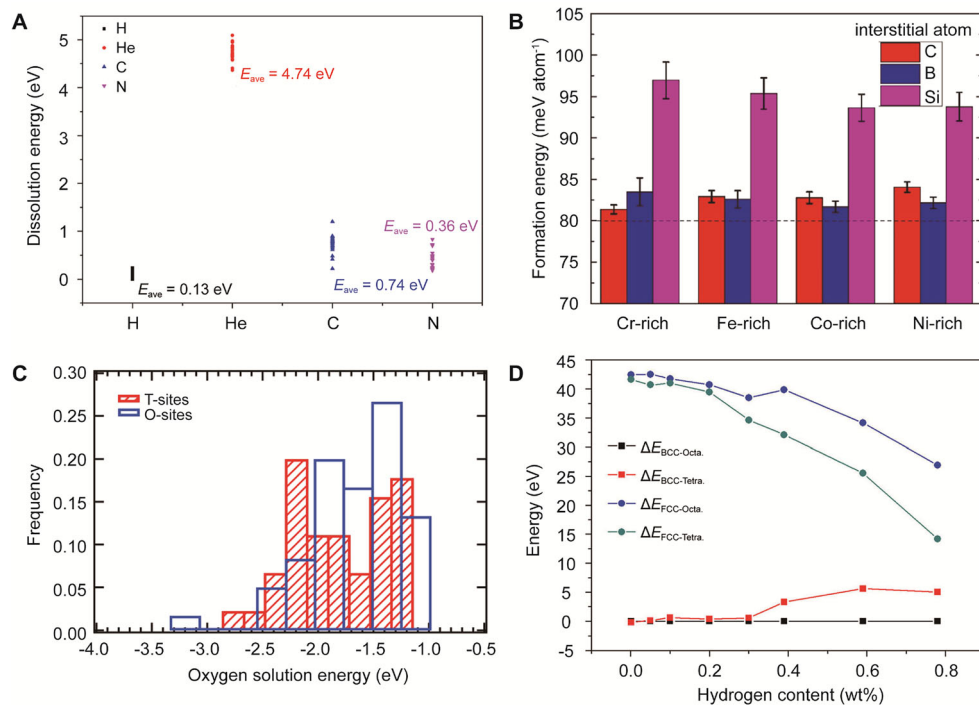


**Fig. 2** **A** Dissolution energies of hydrogen, carbon, and nitrogen for FeCoNiCr. Reproduced with permission from Ref. [17]. Copyright 2020, Japan Institute of Metals and Materials. **B** Formation energies of carbon and boron in different local chemical environments for FeCoNiCr. Reproduced with permission from Ref. [16]. Copyright 2022, Elsevier. **C** Statistical distribution of solution energy for oxygen at different interstitial sites in MoNbTaW. Reproduced with permission from Ref. [19]. Copyright 2020, AIP Publishing. **D** Dissolution energy difference between the octahedral and tetrahedral sites of FCC and BCC structures as a function of hydrogen content in TiZrHfNbMo. Reproduced with permission from Ref. [22]. Copyright 2020, American Chemical Society

result in a wide distribution of H diffusion energy barriers. The site occupancy of hydrogen in HEAs is quite complicated. Some studies suggested that hydrogen favors the tetrahedral sites in alloys such as FCC-TiZrHfMoNb [22], BCC-Ti<sub>23</sub>Cr<sub>25</sub>Ta<sub>23</sub>V<sub>29</sub>, BCC-Ti<sub>27</sub>Cr<sub>27</sub>Ta<sub>18</sub>V<sub>28</sub> [23], and BCC-NbMoTaW [24], whereas some reported that hydrogen prefers to occupy the octahedral sites in BCC-NbTiVZr [25], BCC-TiZrVMoNb [26], BCC-TiZrHfMoNb [22], FCC-TiVNbTa [27], FCC-TiZrVMoNb [26]. The possible reasons for the complicated site occupancy for hydrogen can be threefold: first, the introduction of hydrogen may induce a phase transformation from BCC to FCC structure in refractory HEAs, and hydrogen prefers to occupy the tetrahedral sites in BCC structures but the octahedral sites in FCC structures (Fig. 2D) [22, 26]. Second, hydrogen may occupy both tetrahedral and octahedral sites simultaneously of a structure [25, 27]. Third, the hydrogen occupancy at the octahedral sites is related to the vacancy formation [28]. Although the precise mechanism of this complex site occupancy is still unclear, it is interesting to note that some refractory HEAs show excellent potential for hydrogen storage applications. The hydrogen storage capability can be determined qualitatively from the phonon spectra method by assessing the lattice dynamic stabilities. To date, the reported HEAs with the maximum hydrogen storage capacity is NbTiVZr (2.94 wt%) [25], which is superior to most other BCC HEAs, such as NbTiVZrHf (2.7 wt%), NbMoVZrTi (2.65 wt%) [26], NbMoTiZrHf (1.94 wt%) [22], NbTiZrHfTa (1.68 wt%) [29], TiZrNbTa (1.4 wt%) [30], and MgZrTiFe<sub>0.5</sub>Co<sub>0.5</sub>Ni<sub>0.5</sub> (1.2 wt%) [31]. Moreover, the hydrogen storage capacity of NbTiVZr surpasses that of the well-known hydrogen storage alloy V<sub>20</sub>Ti<sub>28</sub>Cr<sub>52</sub> (2.6 wt%) [32]. These properties position refractory HEAs as promising candidates for future hydrogen storage applications.

In addition to lattice distortion, the solubility and segregation of interstitials are also highly dependent on the inhomogeneous distribution of electrons induced by the chemical effect [24–26]. Numerous studies found that the empirical parameter, valence electron concentration (VEC), combines these two contributions [12, 14, 20, 21], and a high VEC is generally corresponding to a large solubility. Furthermore, the solubility of hydrogen in refractory HEAs was calculated by employing the multi-objective Bayesian optimization-aided DFT calculations [33]; the results suggested that the thermodynamics of the first stage of desorption are determined mostly by the bulk modules, whereas those of the second stage are dominated by the number of states in the d-band. It is worth noting that a high d-band in the second stage that spans more of the Fermi level also exhibits a close dependence on low VECs.

### 3 Local structures and lattice distortion

The high strength of HEAs is considered to be closely related to the severe lattice distortion. Experimentally, the lattice distortion can be measured by using X-ray or neutron diffraction techniques. However, such measurements usually ignore the contribution of chemical fluctuations and provide averaged information over all elements. Similar problems also exist for the empirical parameters, which generally do not consider the electronic and magnetic effects. Recently, a parameter  $\Delta d$  [34] based on DFT calculations was proposed to quantitatively describe the degree of local lattice distortion in HEAs, as expressed by

$$\Delta d = \frac{1}{N} \sum_i^N \sqrt{(x_0 - x_i)^2 + (y_0 - y_i)^2 + (z_0 - z_i)^2} \quad (2)$$

where  $N$  is the total number of interstitial atoms, and  $(x_0, y_0, z_0)$  and  $(x_i, y_i, z_i)$  are the Cartesian coordinate positions of atoms before and after the structural relaxation, respectively. It is found that the local lattice distortion in HEAs increases significantly with increased concentration of interstitials. Taking FeCoNiCr as an example, the fluctuation and magnitude of  $\Delta d$  induced by oxygen interstitials are much larger than those of global lattice distortion [15], as illustrated in Fig. 3A. Similar trends were also observed for carbon [35], nitrogen [36], and hydrogen [24] in FeCoNiCrMn, and carbon [21] and oxygen [20] in refractory HEAs. For conventional HEAs without interstitials, the origin of the local lattice distortion is disputed. Some studies suggested that the local lattice distortion derives mainly from the CSRO induced by the preferable bonding between certain atomic pairs [37], while others argued that the underlying mechanism is related to the charge transfer among constituent elements [38]. For interstitial-containing HEAs, the interaction of interstitial atoms with other host elements can induce the formation of complex CSRO. For example, carbon [12], nitrogen [14], oxygen [39], and hydrogen [40] were found to favor the Cr-rich regions while avoiding Ni-rich regions in FeCoNiCrMn. This additional CSRO was found to directly affect the local lattice distortion. As shown in Fig. 3C, the local bond distortions from of the Cr-rich environment in FeCoNiCrMn become wider for all elements with the addition of nitrogen. Such an effect can be enhanced by further doping carbon [41]. The competition between carbon and nitrogen compels carbon to diffuse from the (Cr,Mn)-enriched regions to the (Co,Fe)-enriched regions.

In addition to CSRO, the formation of OICs is also found to contribute to the local lattice distortion. As displayed in Fig. 3B, the ordered structures show larger lattice distortions compared to the disordered structures, and the degree of lattice distortions keeps nearly unchanged



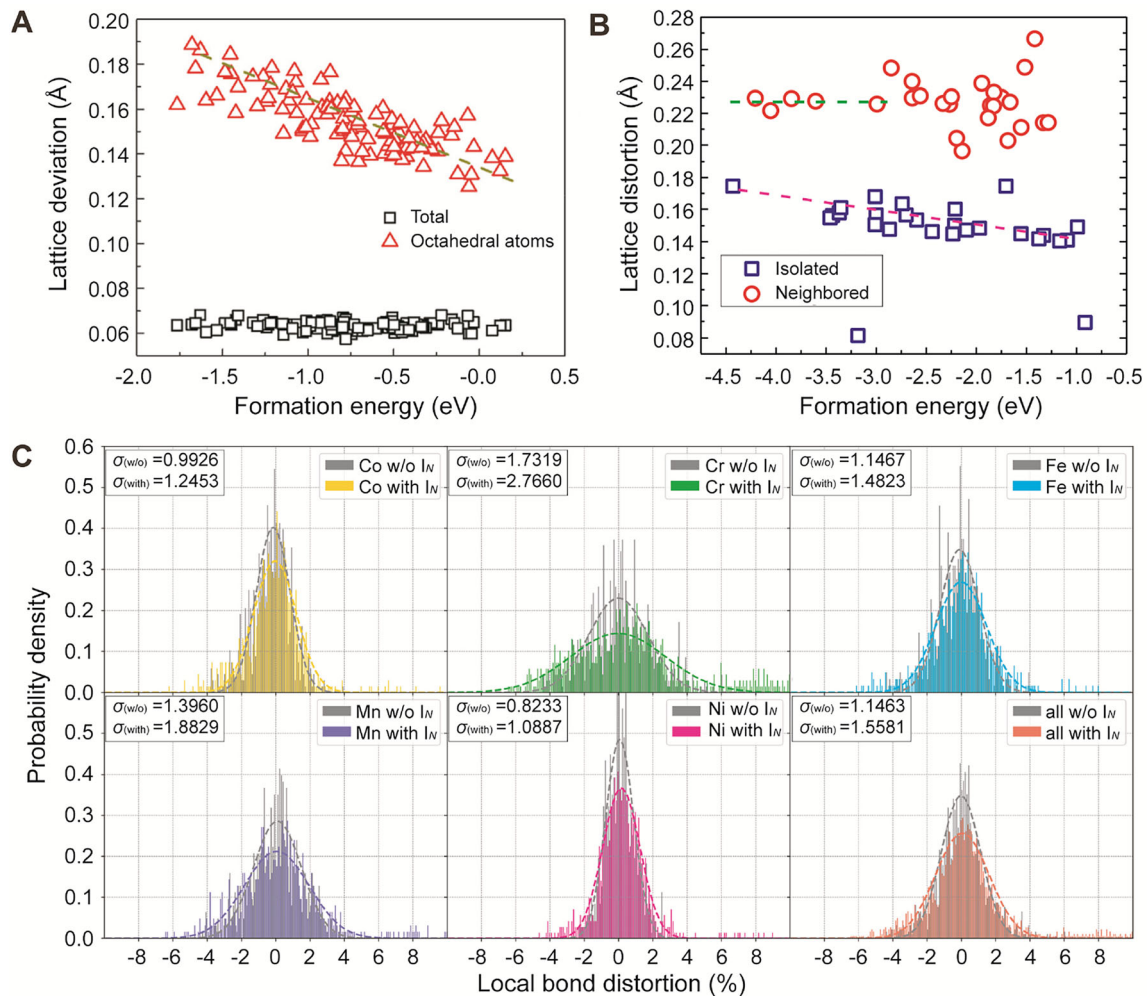


**Fig. 3** **A** Local (triangles in red) and global (squares in black) lattice distortions with oxygen interstitials in FeCoNiCr. Reproduced with permission from Ref. [15]. Copyright 2020, Elsevier. **B** Local lattice distortions of ordered ('neighbored', circles in red) and disordered ('isolated', squares in blue) structures in FeCoNiCr with quadruple oxygen interstitials. Reproduced with permission from Ref. [15]. Copyright 2020, Elsevier. **C** Local lattice distortions with and without nitrogen interstitials for Cr-rich environment in FeCoNiCrMn. Reproduced with permission from Ref. [36]. Copyright 2021, Elsevier

responding to the variation of formation energies. It suggests that the OICs can be stable in oxygen-containing FeCoNiCr, which arouses severe lattice distortions [15, 41]. Since these local distortions break the high symmetry of interstitial positions and show strongly anisotropy strains, the resulted strengthening effect is more pronounced than that from substitutional solid solutions that typically have spherically symmetric stress fields. Zhou et al. [42] found that carbon-ordered structures can effectively inhibit dislocation motion, significantly enhancing the strength and hardness of alloys, while the stress field of dislocations can substantially increase the degree of ordering of within structures. Notably, OICs are frequently reported in refractory HEAs via adjusting the composition of CSRO regions [9, 43, 44]. Zhou et al. [45] found that the presence of OICs can significantly increase the critical shear stress needed for continuous dislocation

movement, with a pinning-cutting behavior observed when an edge dislocation encounters an OIC, and a cross-slip behavior occurring when a screw dislocation encounters an OIC. Unlike FeCoNiCrMn systems, refractory HEAs often have multiple types of CSRO regions. For instance, in HfNbTiZr, some CSRO regions are enriched in Ti and Zr and some are enriched in Hf and Ta. While the energy distributions for different regions are similar, both carbon and oxygen are found to favor Ti-enriched regions and dislike Nb-enriched regions [20, 21]. This result was further confirmed by the mean square displacement (MSD) based on molecular dynamics calculations. It was found that the MSD slope corresponding to Nb is much larger than that to other elements, indicating a large diffusion rate and unstable binding of Nb–O pairs. Therefore, decreasing the Nb content and increasing the concentration of

interstitials may be an efficient approach to introduce OICs in refractory HEAs.

The intrinsic origin for CSRO and OICs associated with local lattice distortion is attributed to the large difference between the interstitials and surrounding metallic elements in charge transfer [35]. The addition of oxygen and nitrogen in NbHfTiZr lowers the Bader charges of metallic atoms, because they can attract electrons from local environments [46]. This allows the original metal–metal bond to transform into ionic-like metal–interstitial bonds, thus enhancing the atomic cohesion. Moreover, some studies suggested that the charge transfer between atomic pairs is highly related to the magnetic moments of atoms by changing their unpaired spins [17]. In FeCoNiCrMn HEAs, it is found that the magnetic moments of Cr are increased near the interstitials, while those of other elements are decreased. The order of change is related to the effects of interstitials on charge transfer and bond lengths. The charge transfer potency of interstitials is found to follow the order of  $N > C > B > H$  in FeCoNiCr [16, 17].

## 4 Effect of interstitials on defect structures and energetics

### 4.1 Interstitial effects on vacancies

Vacancies are inevitable defects for metallic materials upon preparation or irradiation. They usually play multiple roles in affecting mechanical behaviors through facilitating atom diffusion, activating dislocation nucleation, hindering dislocation motion, and/or inducing crack initiation. It is found that the formation of monovacancies in FeCoNiCrMn is more difficult than the constituent elemental metals [47]. The addition of hydrogen significantly decreases the formation energy of vacancies and stabilizes the hydrogen–vacancy complex. The reason is ascribed to the charge transfer from metallic elements to their neighboring hydrogen atoms, which reduces the mean free path of electrons and energy dissipation rates. Upon deformation, the neighboring monovacancies can aggregate and grow into multi-vacancy clusters. Using the hydrogen enhanced vacancy stabilization model, Wang et al. [47] found that the binding energies of vacancies and hydrogen–vacancy complex in different local chemical environments are all negative for FeCoNiCrMn (Fig. 4A), indicating that the growth and coalescence of vacancies are spontaneous. Nevertheless, their growth behavior can be hindered in some cases when hydrogen is trapped (the dashed circles), which avoids the formation of large clusters. Besides, the growth rate of vacancies in FeCoNiCrMn is found to be lower than that in pure Fe and Ni, as shown in Fig. 4B.

These results suggest that multicomponent HEAs may yield exceptional resistance to hydrogen embrittlement.

Regarding boron interstitials, Wang et al. [48] calculated the vacancy formation energy of B-doped AlCrMoNbZr HEAs while considering different local chemical environments. They found no clear pattern in the vacancy formation energy relative to the variety and number of atoms in the local chemical environment, which can be attributed to the significant lattice distortion caused by boron doping. Consequently, the increase in the average vacancy formation energy in B-doped HEAs facilitates vacancy formation, which is not conducive to enhancing the initial irradiation resistance performance. As for carbon interstitials, the vacancy migration energy is significantly increased in Fe<sub>49.5</sub>Mn<sub>30</sub>Co<sub>10</sub>Cr<sub>10</sub>C<sub>0.5</sub> HEAs [35]. The values are weak negative related to the average metallic radii of the local surrounding environment [28, 49] but associated with the magnetic states and chemical compositions. In Fe<sub>50</sub>Mn<sub>30</sub>Co<sub>10</sub>Cr<sub>10</sub>, the vacancy migration energy for carbon interstitials follows the order of  $Co > Fe > Mn > Cr$  [35], leading to nanoscale localized elemental fluctuations and often implying stronger local lattice distortion. As a result, the carbon interstitials hinder the vacancy diffusion and increase the local lattice distortion, thereby enhancing the recombination of radiation-induced point defects and inhibiting irradiation hardening [35].

### 4.2 Interstitial effects on generalized SFs

The plastic deformation behavior of HEAs is highly dependent upon their stacking fault energies (SFEs). Generally, a low SFE ( $< 20 \text{ mJ m}^{-2}$ ) leads to martensitic transformation, while a high SFE ( $> 40 \text{ mJ m}^{-2}$ ) results in dislocation gliding and shear banding, and SFEs in the range of  $20\text{--}40 \text{ mJ m}^{-2}$  can induce deformation twinning [50]. The calculated SFEs of equimolar FeCoNiCrMn HEAs are in the range of  $-93$  to  $-5 \text{ mJ m}^{-2}$  at 0 K [51], suggesting that the dominant deformation mechanism is the martensite transformation at this temperature. It is found that doping hydrogen to HEAs [8, 13] decreases the SFEs, while adding carbon [12] and nitrogen [14, 52] to HEAs increases the SFEs. In conventional FCC alloys, it is generally recognized that carbon increases the SFEs, whereas the effect of nitrogen on SFEs can vary, either increasing, decreasing, or having minimal effects, depending on the specific alloy compositions. Many studies suggested that the excellent resistance to hydrogen embrittlement for FeCoNiCrMn is related to the reduced SFEs by hydrogen, which induces the formation of nanotwins and SFs [53]. Zhu et al. [8] found that the addition of hydrogen reduces the energy barrier for twin nucleation by using first-principles calculations. Their experimental observations confirmed that a higher density of deformation twins was

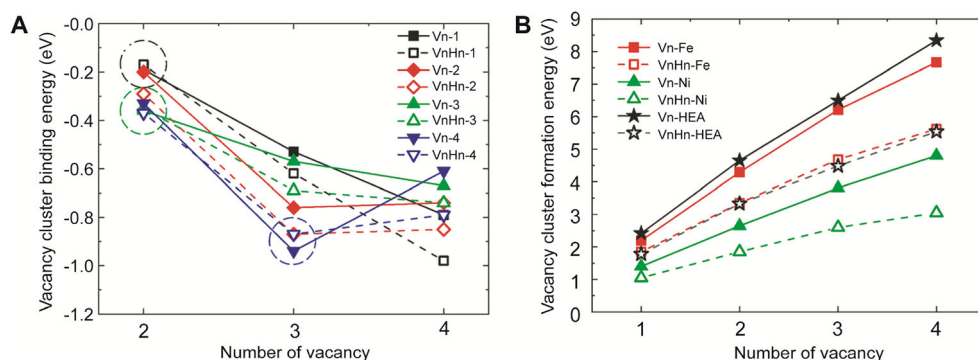


**Fig. 4** **A** Binding energies of vacancy clusters and hydrogen-vacancy clusters at different positions in FeCoNiCrMn; **B** formation energies of vacancy clusters and hydrogen-vacancy clusters in pure Fe and Ni and FeCoNiCrMn. Reproduced with permission from Ref. [47]. Copyright 2022, Elsevier

generated in the FeCoNiCrMn HEAs under a lower hydrogen concentration environment, resulting in a larger strength and a higher ductility after hydrogen charging. Luo et al. [54] experimentally found that while hydrogen alloying does not increase the yield strength of FeCoNiCrMn HEAs, it does enhance the strain-hardening rate. This indicates that the beneficial effect of nanotwins on strain hardening primarily improves both strength and ductility.

Carbon and nitrogen are found to increase the SFE of HEAs, which turns the TRIP into TWIP, sometimes even dislocation slips, depending on the content of soluble interstitials. Specifically, as shown in Fig. 5A, B, the increase of SFE is qualitatively evaluated as  $8 \text{ mJ m}^{-2}$  for 1 at% of nitrogen [14], which is close to that of carbon ( $7 \text{ mJ m}^{-2}$ ) [12]. However, they exhibit distinct effects on the deformation behavior of FeCoNiCrMn HEAs. Nitrogen is found to provide solid solution strengthening effect but has little impact on the deformation mode [55], whereas carbon is reported to trigger such deformation mechanisms as phase transformation, deformation twinning, and dislocation slip [10, 56]. Li et al. constructed various configurations for nitrogen-containing FeCoNiCrMn HEAs and found that there is an average increased SFE of approximately  $147 \text{ mJ m}^{-2}$  [52] for 1 at% nitrogen. Notably, Chen et al. recently found that the SFE of  $\text{Fe}_{50}\text{Mn}_{30}\text{Co}_{10}\text{Cr}_{10}$  presents a sophisticated dependence on the concentration of nitrogen, as the structure of  $(\text{Fe}_{50}\text{Mn}_{30}\text{Co}_{10}\text{Cr}_{10})_{100-x}\text{N}_x$  evolves from a single FCC-to-FCC + HCP dual phase, and ultimately reverts to a predominantly FCC phase with increasing nitrogen [57]. Additionally, carbon shows an obvious anti-Suzuki behavior, which tends to diffuse away from the SF planes in FeCoNiCrMn [12], similar to that in  $\gamma$ -Fe and TWIP steels [58]. As displayed in Fig. 5D, the ratios of local carbon in the vicinity of SFs and in the bulk region are all less than 1 within the temperature range of 0–2,000 K. Typically, the addition of carbon increases the

SFEs of FCC alloys, such as TWIP steels, Fe–Mn–C–Al steels, and Cantor alloy and its derivatives, resulting in a reduced tendency for twinning. Li et al. [56] experimentally observed that the density of nanotwins decreases as the carbon content increases from 0 to 0.8 at% in CoCr–FeMnNi HEAs at room temperature. Meanwhile, the interstitial HEA with 0.8 at% carbon exhibits more than five times the yield strength of the C-free reference alloy. The significant increase in strength can be attributed to the substantial interstitial solid solution strengthening, which is related to the strong interactions between interstitial carbon and dislocations. Importantly, tuning the SFE of alloys through interstitials provides an effective method for precisely designing their deformation mode. For example, adding approximately 0.5 at% carbon to a non-equiatomic TRIP-assisted dual-phase HEA results in the combined activation of TWIP and TRIP effects [59].

#### 4.3 Interstitial effects on GBs

GBs also play an important role in controlling mechanical properties and deformation behavior of HEAs. Based on DFT calculations, Guan et al. investigated the segregation behavior of hydrogen at  $\Sigma 3(111)$  GBs of CoNiCr and FeCoNiCr alloys [60]. It is found that the solution energies of hydrogen at GBs of CoNiCr are higher than those in the bulk, suggesting that hydrogen is hard to segregate to GBs. The reason is ascribed mainly to the existence of Cr, which shrinks the charge density isosurface and limits the movement of neighboring hydrogen atoms. Moreover, the dipole moment interaction between Cr and hydrogen compels hydrogen atoms at interstitial sites away from each other, which improves the resistance to hydrogen embrittlement. Nevertheless, the introduction of Fe weakens this suppression effect, improves the solubility of hydrogen at GBs, and alters the diffusion process of hydrogen. The negative solution energies and low binding

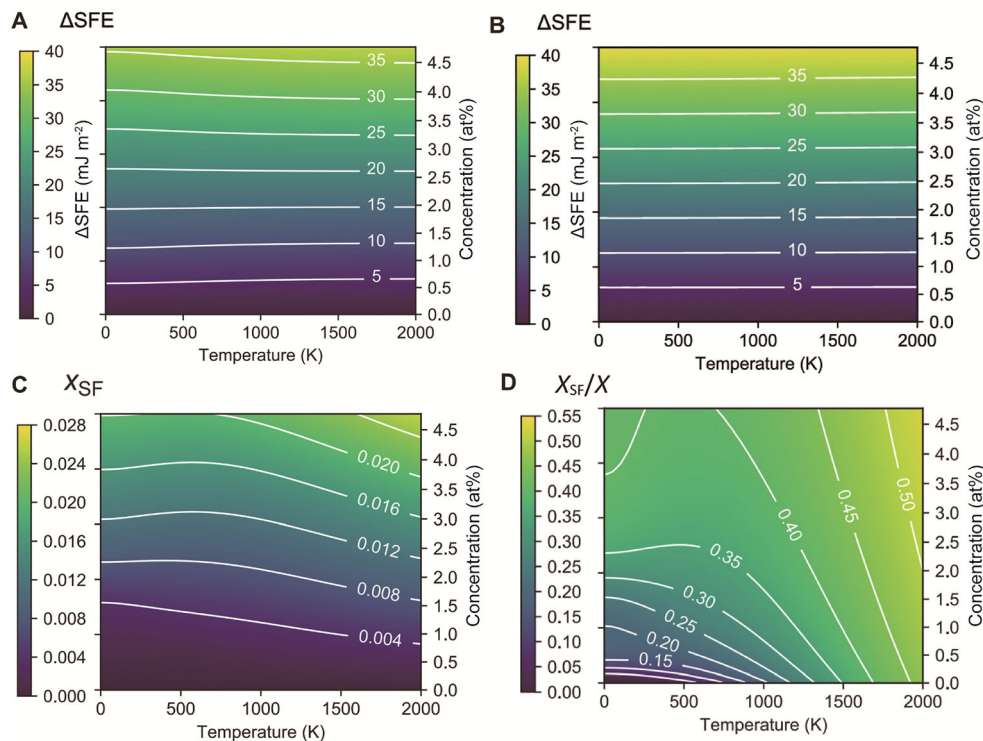


**Fig. 5** Impacts of **A** carbon and **B** nitrogen on the SFEs of FeCoNiCrMn as a function of temperature and concentration. Reproduced with permission from Ref. [12]. Copyright 2019, American Physical Society and Ref. [14]. Copyright 2021, Springer. **C** Ratios of the number of carbon atoms to that of available interstitial sites at the stacking faults ( $X_{SF}$ ) as a function of temperature and carbon ratio in the bulk region ( $X$ ), and **D** ratios of  $X_{SF}$  to  $X$  for FeCoNiCrMn HEAs. Reproduced with permission from Ref. [12]. Copyright 2019, American Physical Society

energies of hydrogen in FeCoNiCr suggest that the dissolution of hydrogen at GBs is spontaneous but the interaction among hydrogen atoms is weak. In addition, Fe is found to block the migration channels of hydrogen at GBs while promoting the diffusion of hydrogen from the bulk to GBs. Despite those, the high migration barriers and the large lattice distortion make the diffusion of hydrogen at GBs in FeCoNiCr difficult. By analyzing the density of states (DOS) before and after hydrogen charging, it is found that hydrogen makes little effects on the d electron density of Ni and Co while providing additional flexibility of electron deformation for Cr or Fe.

By using three-dimensional atom probe tomography (3D-APT), Yuan et al. reported that the GBs are concentrated with more than one type of interstitials in TiZrHfNb alloys [61]. The DFT calculations of GB energies for three different  $\Sigma 3(112)[001]$  configurations suggest that the atomic distribution of GBs is not random or uniform, and the structure with Ti and Zr segregation is very stable. The segregation of boron, carbon, and oxygen to GBs can reduce the GB energy and stabilize the GBs, following the order of  $C > O > B$  (Fig. 6A) [61]. Along with the co-segregation of Zr and Ti at GBs, these interstitials cause severer embrittlement. Moreover, oxygen at GBs is

suggested to be the main cause of intergranular cracking in NbMoTaW HEAs [62]. In contrast to the positive strengthening energy of oxygen shown in Fig. 6B, carbon and boron are found to yield negative values at the typical  $\Sigma 5(310)[001]$  GBs, which manifests the enhanced GBs cohesive. In addition, the more negative segregation energies and higher diffusion rate suggest that carbon and boron are more inclined to segregate to GBs. Thus, the introduction of carbon and boron can effectively eliminate the segregation of oxygen at GBs, thereby enhancing the cohesion of GBs. The underlying mechanisms were explained by the results of charge density distribution and the electron localization function (ELF), where the additions of boron and carbon lead to an abundant charge accumulation, strong interaction with adjacent metallic elements, and the transformation from ionic to metallic bond (Fig. 6C). The enhanced GB bonding in the B/C-doped HEAs significantly inhibits crack initiation at GBs. Consequently, crack propagation becomes more challenging due to the higher energy barrier and the complex interactions with the distorted lattice. As a result, the deformability of the B/C-doped HEAs is dramatically enhanced [61].



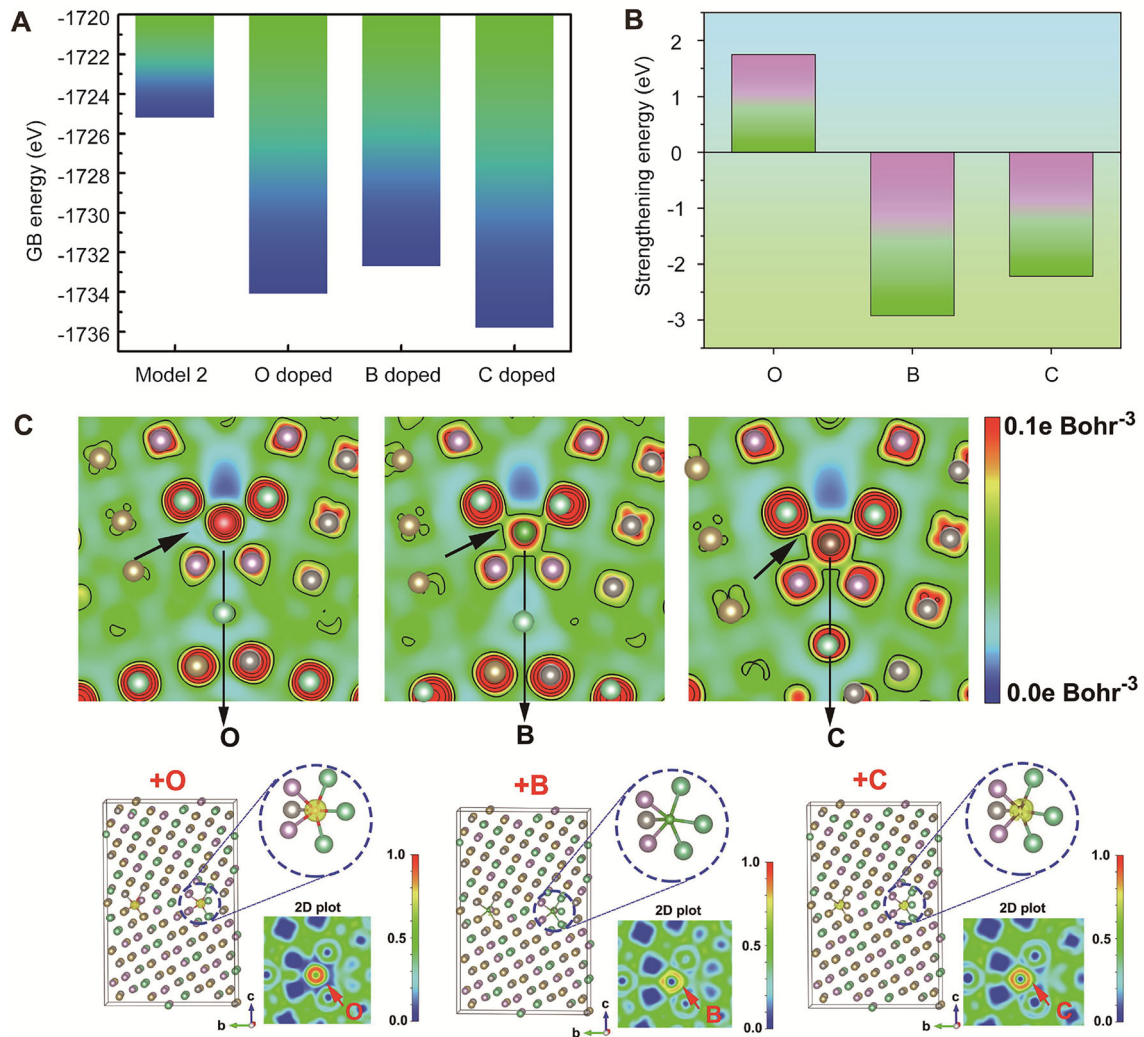


**Fig. 6** **A** GB energies of  $\Sigma 3(112)[011]$ GBs for TiZrHfNb with and without oxygen, boron, and carbon. Reproduced with permission from Ref. [61]. Copyright 2023, Elsevier. **B** Strengthening energies and **C** charge density distribution, ELF of  $\Sigma 5(310)[001]$ GBs for NbMoTaW with oxygen, boron, and carbon. Reproduced with permission from Ref. [62]. Copyright 2022, Elsevier

## 5 Concluding remarks and future outlook

The atomic understanding of interstitial effects in HEAs has been greatly improved by computational modeling and simulations. The interactions of interstitials with constituent elements and defect structures show great potential in tuning mechanical properties of HEAs. The effect of interstitials on the lattice structure of HEAs are analyzed from the solubilities, site preference, bonding, and charge transfer. It is found that the strengthening effects of interstitials are highly depending on local chemical environments. Particularly, the interstitial-induced local lattice distortions and OICs can contribute substantially to the strengthening of HEAs. Moreover, interstitials also have an important impact on the defect structures and associated defect energetics, which can remarkably affect the plastic deformation and fracture behavior of HEAs. Therefore, the

control of interstitials and their interactions with constituent elements and defect structures provides new opportunities for optimizing mechanical properties and deformation behavior of HEAs. Further investigations are required for better understanding and control over properties of interstitial-strengthened HEAs from the theory, experiment, and machine learning aspects (Fig. 7). From a theoretical perspective, it is crucial to gain a deep understanding of the mechanisms behind strengthening and deformation. On the experimental front, it is particularly intriguing to explore how multiple interstitials and ordered structures influence the mechanical properties of interstitial-strengthened HEAs. In parallel, machine learning offers a powerful tool for predicting material properties and discovering new materials.

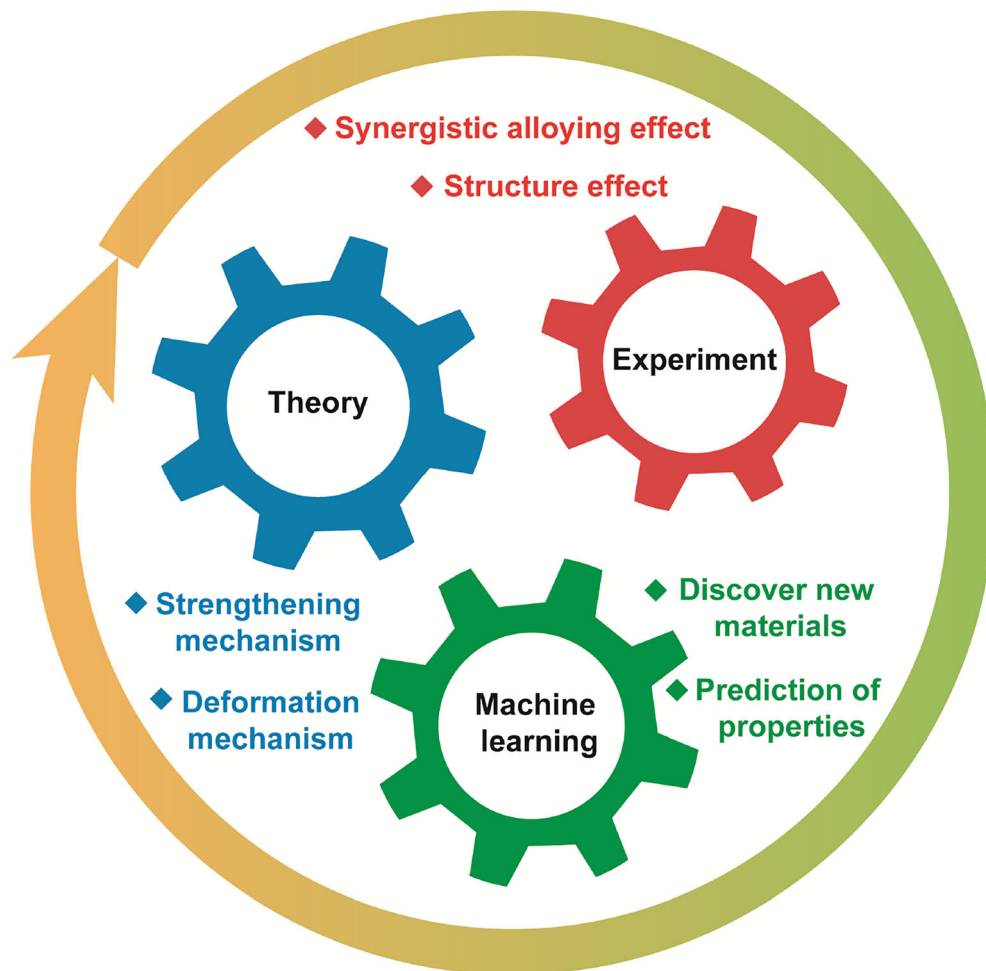


**Fig. 7** Outlook on future research of interstitial-strengthened HEAs

### 5.1 Theoretical analysis and modeling of strengthening and deformation

The interaction of interstitial atoms with dislocations, twins, and SFs is complex and multifaceted. These interactions can significantly influence the deformation behavior of materials, affecting their mechanical properties. As a result, there is a need to develop new theoretical frameworks and models to better understand and predict dislocation activities. Such advancements could lead to improved material design and performance by providing deeper insights into the fundamental mechanisms governing material deformation. Moreover, an accurate evaluation of interstitial solid solution strengthening is crucial for the fundamental understanding of mechanical properties of HEAs. However, classical models, such as Fleischer and Labusch models, are found not accurate enough to describe the relationship between the concentration of interstitials and increased yield strength of HEAs [63]. These models often rely on parameters like lattice mismatch and shear modulus mismatch, which are not well-defined or sufficient

for complex HEAs. Moreover, additional factors, such as severe lattice distortion, complex phase interactions, and non-linear effects, might also influence the strengthening effect. Thus, it is vital to establish a physical model suitable for interstitial-strengthened HEAs for a better understanding of and eventually control over the interstitial solid solution strengthening in HEAs.

### 5.2 Mechanistic understanding of alloying and structure effects

Due to the severe lattice distortion, HEAs can usually absorb more than one type of interstitials. Recent findings suggest that the mechanical properties of HEAs can be efficiently tuned by co-doping of multiple interstitials. For example, the synergy of interstitial carbon and nitrogen in FeCoNiCr is found to significantly enhance the maximum shear stress [64]. Additionally, the competition between carbon and hydrogen is found to suppress the hydrogen trapping at GBs, thereby alleviating the hydrogen embrittlement [65]. However, the synergistic effects of multi-interstitials and their

interactions on the mechanical properties of HEAs are quite complicated and remain to be elucidated an in-depth understanding of which would facilitate the design of novel alloys with superior properties.

In addition to disordered HEAs, interstitials have also been utilized in some ordered multicomponent alloys. A typical example is an FCC/L1<sub>2</sub> Ni<sub>43.9</sub>Co<sub>22.4</sub>-Fe<sub>8.8</sub>Al<sub>10.7</sub>Ti<sub>11.7</sub>B<sub>2.5</sub> alloy [66], in which a disorder layer enriched in Fe, Co, and boron is formed at GBs. This layer allows for the dislocation transmission across GBs, thus resulting in excellent combination of high strength and ductility. Inspired by these exciting results, a fundamental understanding of the interstitial effects on the structure and properties of ordered multicomponent alloys, such as L1<sub>2</sub>, B2, L1<sub>0</sub>, and L2<sub>1</sub> alloys, may provide tremendous opportunities for developing strong-yet-ductile ordered intermetallic alloys.

### 5.3 Machine learning of interstitial-strengthened HEAs

Available data suggest that a change in interstitial type and concentration may bring a significant variation in the phase stability and deformation behavior of HEAs. Thus, the exploration of unexplored composition space in interstitial-strengthened HEAs is urgently needed. Recently, the combination of machine learning and DFT calculations has attracted increasing interest from researchers, which has been successfully applied to accelerate the discovery of some novel interstitial-strengthened HEAs [18, 33], demonstrating high capability in predicting mechanical properties and guiding the design of new high-performance HEAs. In addition, machine learning can also be utilized to develop the interatomic potentials for the Monte Carlo-Molecular Dynamics (MC-MD) method with a large atomic scale. Specifically, deep learning potentials, trained on extensive datasets, can capture the nuanced behaviors of atoms in these alloys with high precision. This advanced approach allows researchers to integrate MD simulations with deep learning potentials, enabling more accurate and efficient predictions of various material properties. By leveraging the computational power and adaptability of deep learning, scientists can overcome previous limitations and unlock the full potential of HEAs in various applications.

**Acknowledgements** The authors acknowledge the financial support from National Natural Science Foundation of China (No. 52171162), Research Grants Council of Hong Kong (Nos. 15202824, 15227121, C5002-24Y, C1017-21GF, and C1020-21GF), Shenzhen Science and Technology Program (No. JCYJ20210324142203009), the Research Institute for Advanced Manufacturing Fund (No. P0046108), PolyU Fund (Nos. P0044243 and P0043467), and Guangdong Science and Technology Innovation Foundation (No. 2023A1515240061).

**Funding** Open access funding provided by The Hong Kong Polytechnic University.

**Author contributions** Qiang Yu and Shi Qiu conceived and designed the project. Zeng-Bao Jiao supervised the project. All authors contributed to the analysis and the writing of the manuscript.

**Data availability** The data that support the findings of this study are available from the corresponding author upon reasonable request.

### Declarations

**Conflict of interests** The authors declare that they have no conflict of interest.

**Open Access** This article is licensed under a Creative Commons Attribution 4.0 International License, which permits use, sharing, adaptation, distribution and reproduction in any medium or format, as long as you give appropriate credit to the original author(s) and the source, provide a link to the Creative Commons licence, and indicate if changes were made. The images or other third party material in this article are included in the article's Creative Commons licence, unless indicated otherwise in a credit line to the material. If material is not included in the article's Creative Commons licence and your intended use is not permitted by statutory regulation or exceeds the permitted use, you will need to obtain permission directly from the copyright holder. To view a copy of this licence, visit <http://creativecommons.org/licenses/by/4.0/>.

### References

- [1] Hsu WL, Tsai CW, Yeh AC, Yeh JW. Clarifying the four core effects of high-entropy materials. *Nat Rev Chem*. 2024;8(6): 471–85. <https://doi.org/10.1038/s41570-024-00602-5>.
- [2] Zhang WT, Wang XQ, Zhang FQ, Cui XY, Fan BB, Guo JM, Guo ZM, Huang R, Huang W, Li XB, Li MR, Ma Y, Shen ZH, Sun YG, Wang DZ, Wang FY, Wang LQ, Wang N, Wang TL, Wang W, Wang XY, Wang YH, Yu FJ, Yin YZ, Zhang LK, Zhang Y, Zhang JY, Zhao Q, Zhao YP, Zhu XD, Sohail Y, Chen YN, Feng T, Gao QL, He HY, Huang YJ, Jiao ZB, Ji H, Jiang Y, Li Q, Li XM, Liao WB, Lin HJ, Liu H, Liu Q, Liu QF, Liu WD, Liu XJ, Lu Y, Lu YP, Ma W, Miao XF, Pan J, Wang Q, Wu HH, Wu Y, Yang T, Yang WM, Yu Q, Zhang JY, Chen ZG, Mao L, Ren Y, Shen BL, Wang XL, Jia Z, Zhu H, Wu ZD, Lan S. Frontiers in high entropy alloys and high entropy functional materials. *Rare Met*. 2024;43(10):4639–776. <https://doi.org/10.1007/s12598-024-02852-0>.
- [3] He MY, Shen YF, Jia N, Liaw PK. C and N doping in high-entropy alloys: a pathway to achieve desired strength-ductility synergy. *Appl Mater Today*. 2021;25:101162. <https://doi.org/10.1016/j.apmt.2021.101162>.
- [4] Zhu C, Xu L, Liu M, Guo M, Wei S. A review on improving mechanical properties of high entropy alloy: interstitial atom doping. *J Mater Res Technol*. 2023;24:7832–51. <https://doi.org/10.1016/j.jmrt.2023.05.002>.
- [5] Belcher CH, MacDonald BE, Apelian D, Lavernia EJ. The role of interstitial constituents in refractory complex concentrated alloys. *Prog Mater Sci*. 2023;137:101140. <https://doi.org/10.1016/j.pmatsci.2023.101140>.
- [6] Cottrell AH. Unified theory of effects of segregated interstitials on grain boundary cohesion. *Mater Sci Technol*. 2013;6(9): 806–10. <https://doi.org/10.1179/mst.1990.6.9.806>.

- [7] Chen S, Rana R, Haldar A, Ray RK. Current state of Fe–Mn–Al–C low density steels. *Prog Mater Sci.* 2017;89:345–91. <https://doi.org/10.1016/j.pmatsci.2017.05.002>.
- [8] Zhu T, Zhong ZH, Ren XL, Song YM, Ye FJ, Wang QQ, Ngan AHW, Wang BY, Cao XZ, Xu Q. Influence of hydrogen behaviors on tensile properties of equiatomic FeCrNiMnCo high-entropy alloy. *J Alloy Compd.* 2022;892:162260. <https://doi.org/10.1016/j.jallcom.2021.162260>.
- [9] Lei Z, Liu X, Wu Y, Wang H, Jiang S, Wang S, Hui X, Wu Y, Gault B, Kontis P, Raabe D, Gu L, Zhang Q, Chen H, Wang H, Liu J, An K, Zeng Q, Nieh TG, Lu Z. Enhanced strength and ductility in a high-entropy alloy via ordered oxygen complexes. *Nature.* 2018;563(7732):546–50. <https://doi.org/10.1038/s41586-018-0685-y>.
- [10] Su J, Raabe D, Li Z. Hierarchical microstructure design to tune the mechanical behavior of an interstitial TRIP-TWIP high-entropy alloy. *Acta Mater.* 2019;163:40–54. <https://doi.org/10.1016/j.actamat.2018.10.017>.
- [11] Su J, Wu X, Raabe D, Li Z. Deformation-driven bidirectional transformation promotes bulk nanostructure formation in a metastable interstitial high entropy alloy. *Acta Mater.* 2019;167:23–39. <https://doi.org/10.1016/j.actamat.2019.01.030>.
- [12] Ikeda Y, Tanaka I, Neugebauer J, Körmann F. Impact of interstitial C on phase stability and stacking-fault energy of the CrMnFeCoNi high-entropy alloy. *Phys Rev Mater.* 2019;3(11):113603. <https://doi.org/10.1103/PhysRevMaterials.3.113603>.
- [13] Xie Z, Wang Y, Lu C, Dai L. Sluggish hydrogen diffusion and hydrogen decreasing stacking fault energy in a high-entropy alloy. *Mater Today Commun.* 2021;26:101902. <https://doi.org/10.1016/j.mtcomm.2020.101902>.
- [14] Ikeda Y, Körmann F. Impact of N on the stacking fault energy and phase stability of FCC CrMnFeCoNi: an ab initio study. *J Phase Equilib Diff.* 2021;42(5):551–60. <https://doi.org/10.1007/s11669-021-00877-x>.
- [15] Liu Y, Zheng GP, Li M. The effects of short-range chemical and structural ordering related to oxygen interstitials on mechanical properties of CrCoFeNi high-entropy alloys: a first-principles study. *J Alloy Compd.* 2020;843:156060. <https://doi.org/10.1016/j.jallcom.2020.156060>.
- [16] Song H, Yu M, Zhang Y, Zhang W, Liu Z, Zhang F, Tian F. First-principle study of interstitial atoms (C, B and Si) in CrFeCoNi high entropy alloy. *Mater Today Commun.* 2022;31:103241. <https://doi.org/10.1016/j.mtcomm.2022.103241>.
- [17] Shi J, Lei Y, Hashimoto N, Isobe S. Doping of interstitials (H, He, C, N) in CrCoFeNi high entropy alloy: a DFT study. *Mater Trans.* 2020;61(4):616–21. <https://doi.org/10.2320/matertrans.MT-MK2019009>.
- [18] Zhou XY, Zhu JH, Wu Y, Yang XS, Lookman T, Wu HH. Machine learning assisted design of FeCoNiCrMn high-entropy alloys with ultra-low hydrogen diffusion coefficients. *Acta Mater.* 2022;224:117535. <https://doi.org/10.1016/j.actamat.2021.117535>.
- [19] Samin AJ. A computational investigation of the interstitial oxidation thermodynamics of a Mo–Nb–Ta–W high entropy alloy beyond the dilute regime. *J Appl Phys.* 2020;128(21):215101. <https://doi.org/10.1063/5.0028977>.
- [20] Chen A, Pan Y, Dai J, Fu W, Song X. Theoretical study on the element distribution characteristics and the effects of oxygen in TiZrHfNb high entropy alloys. *Mater Today Commun.* 2023;36:106922. <https://doi.org/10.1016/j.mtcomm.2023.106922>.
- [21] Casillas-Trujillo L, Jansson U, Sahlberg M, Ek G, Nygård MM, Sørby MH, Hauback BC, Abrikosov IA, Alling B. Interstitial carbon in bcc HfNbTiVZr high-entropy alloy from first principles. *Phys Rev Mater.* 2020;4(12):123601. <https://doi.org/10.1103/PhysRevMaterials.4.123601>.
- [22] Hu J, Zhang J, Xiao H, Xie L, Shen H, Li P, Zhang J, Gong H, Zu X. A density functional theory study of the hydrogen absorption in high entropy alloy TiZrHfMoNb. *Inorg Chem.* 2020;59(14):9774–82. <https://doi.org/10.1021/acs.inorgchem.0c00989>.
- [23] Song Z, Ru J, Ma R, Wan M, Zhou J, Xie Q. First-principles studies of behavior of hydrogen and mechanical properties of TiCrTaV high-entropy alloys. *Mater Today Commun.* 2023;35:105929. <https://doi.org/10.1016/j.mtcomm.2023.105929>.
- [24] Ren XL, Shi PH, Yao BD, Wu L, Wu XY, Wang YX. Hydrogen solution in high-entropy alloys. *Phys Chem Chem Phys.* 2021;23(48):27185–94. <https://doi.org/10.1039/d1cp04151g>.
- [25] Gong J, Li Y, Song X, Wang Y, Chen Z. Hydrogen storage of high entropy alloy NbTiVZr and its effect on mechanical properties: a first-principles study. *Vacuum.* 2024;219:112754. <https://doi.org/10.1016/j.vacuum.2023.112754>.
- [26] Hu J, Zhang J, Xiao H, Xie L, Sun G, Shen H, Li P, Zhang J, Zu X. A first-principles study of hydrogen storage of high entropy alloy TiZrVMoNb. *Int J Hydrogen Energy.* 2021;46(40):21050. <https://doi.org/10.1016/j.ijhydene.2021.03.200>.
- [27] Hu J, Zhang J, Li M, Zhang S, Xiao H, Xie L, Sun G, Shen H, Zhou X, Li X, Li P, Zhang J, Vitos L, Zu X. The origin of anomalous hydrogen occupation in high entropy alloys. *J Mater Chem A.* 2022;10(13):7228–37. <https://doi.org/10.1039/d1ta10649j>.
- [28] Moore CM, Wilson JA, Rushton MJD, Lee WE, Astbury JO, Middleburgh SC. Hydrogen accommodation in the TiZrNbHfTa high entropy alloy. *Acta Mater.* 2022;229:117832. <https://doi.org/10.1016/j.actamat.2022.117832>.
- [29] Zlotea C, Sow MA, Ek G, Couzinié JP, Perrière L, Guillot I, Bourgon J, Møller KT, Jensen TR, Akiba E, Sahlberg M. Hydrogen sorption in TiZrNbHfTa high entropy alloy. *J Alloy Compd.* 2019;775:667–74. <https://doi.org/10.1016/j.jallcom.2018.10.108>.
- [30] Zhang C, Song A, Yuan Y, Wu Y, Zhang P, Lu Z, Song X. Study on the hydrogen storage properties of a TiZrNbTa high entropy alloy. *Int J Hydrogen Energy.* 2020;45(8):5367–74. <https://doi.org/10.1016/j.ijhydene.2019.05.214>.
- [31] Zepón G, Leiva DR, Strozi RB, Bedoch A, Figueroa SJA, Ishikawa TT, Botta WJ. Hydrogen-induced phase transition of MgZrTiFe<sub>0.5</sub>Co<sub>0.5</sub>Ni<sub>0.5</sub> high entropy alloy. *Int J Hydrogen Energy.* 2018;43(3):1702–8. <https://doi.org/10.1016/j.ijhydene.2017.11.106>.
- [32] Kong HY, Xie QF, Wu CL, Wang Y, Chen YG, Li HW, Yan YG. Vanadium-based alloy for hydrogen storage: a review. *Rare Met.* 2024;43(12):6201–32. <https://doi.org/10.1007/s12598-024-02839-x>.
- [33] Halpren E, Yao X, Chen ZW, Singh CV. Machine learning assisted design of BCC high entropy alloys for room temperature hydrogen storage. *Acta Mater.* 2024;270:119841. <https://doi.org/10.1016/j.actamat.2024.119841>.
- [34] Song H, Tian F, Hu QM, Vitos L, Wang Y, Shen J, Chen N. Local lattice distortion in high-entropy alloys. *Phys Rev Mater.* 2017;1(2):023404. <https://doi.org/10.1103/PhysRevMaterials.1.023404>.
- [35] Su Z, Shi T, Yang J, Shen H, Li Z, Wang S, Ran G, Lu C. The effect of interstitial carbon atoms on defect evolution in high entropy alloys under helium irradiation. *Acta Mater.* 2022;233:117955. <https://doi.org/10.1016/j.actamat.2022.117955>.
- [36] Lu E, Zhao J, Makkonen I, Mizohata K, Li Z, Hua M, Djurabekova F, Tuomisto F. Enhancement of vacancy diffusion by C and N interstitials in the equiatomic FeMnNiCoCr high entropy alloy. *Acta Mater.* 2021;215:117093. <https://doi.org/10.1016/j.actamat.2021.117093>.
- [37] Zhang FX, Zhao S, Jin K, Xue H, Velisa G, Bei H, Huang R, Ko JYP, Pagan DC, Neuefeind JC, Weber WJ, Zhang Y. Local structure and short-range order in a NiCoCr solid solution alloy.



- Phys Rev Lett. 2017;118(20):205501. <https://doi.org/10.1103/PhysRevLett.118.205501>.
- [38] Oh HS, Obadrak K, Ikeda Y, Mu S, Körmann F, Sun CJ, Ahn HS, Yoon KN, Ma D, Tasan CC, Egami T, Park ES. Element-resolved local lattice distortion in complex concentrated alloys: an observable signature of electronic effects. *Acta Mater.* 2021;216:117135. <https://doi.org/10.1016/j.actamat.2021.117135>.
  - [39] Liu Y, Zheng GP. Interstitial-oxygen induced and magnetically driven HCP-to-FCC transformation in CoCrFeNiO<sub>x</sub> high-entropy alloy: a first-principles study. *Philos Mag.* 2023;103(23):2123–40. <https://doi.org/10.1080/14786435.2023.2265844>.
  - [40] Marques SC, Castilho AV, Dos Santos DS. Effect of alloying elements on the hydrogen diffusion and trapping in high entropy alloys. *Scr Mater.* 2021;201:113957. <https://doi.org/10.1016/j.scriptamat.2021.113957>.
  - [41] Su Z, Ding J, Song M, Jiang L, Shi T, Li Z, Wang S, Gao F, Yun D, Ma E, Lu C. Enhancing the radiation tolerance of high-entropy alloys via solute-promoted chemical heterogeneities. *Acta Mater.* 2023;245:118662. <https://doi.org/10.1016/j.actamat.2022.118662>.
  - [42] Zhou XY, Wu HH, Zhang J, Ye S, Lookman T, Mao X. Unveiling the mechanism of carbon ordering and martensite tetragonality in Fe–C alloys via deep-potential molecular dynamics simulations. *J Mater Sci Technol.* 2025;223:91–103. <https://doi.org/10.1016/j.jmst.2024.10.020>.
  - [43] Jiao M, Lei Z, Wu Y, Du J, Zhou XY, Li W, Yuan X, Liu X, Zhu X, Wang S, Zhu H, Cao P, Liu X, Zhang X, Wang H, Jiang S, Lu Z. Manipulating the ordered oxygen complexes to achieve high strength and ductility in medium-entropy alloys. *Nat Commun.* 2023;14(1):806. <https://doi.org/10.1038/s41467-023-36319-0>.
  - [44] Lei Z, Wu Y, He J, Liu X, Wang H, Jiang S, Gu L, Zhang Q, Gault B, Raabe D, Lu Z. Snoek-type damping performance in strong and ductile high-entropy alloys. *Sci Adv.* 2020;6(25):eaba7802. <https://doi.org/10.1126/sciadv.aba7802>.
  - [45] Zhou XY, Wu HH, Wu Y, Liu X, Peng X, Hou S, Lu Z. Formation and strengthening mechanism of ordered interstitial complexes in multi-principle element alloys. *Acta Mater.* 2024;281:120364. <https://doi.org/10.1016/j.actamat.2024.120364>.
  - [46] Ye YX, Ouyang B, Liu CZ, Duscher GJ, Nieh TG. Effect of interstitial oxygen and nitrogen on incipient plasticity of NbTiZrHf high-entropy alloys. *Acta Mater.* 2020;199:413–24. <https://doi.org/10.1016/j.actamat.2020.08.065>.
  - [47] Wang C, Han K, Liu X, Zhu Y, Liang S, Zhao L, Huang M, Li Z. First-principles study of hydrogen-vacancy interactions in CoCrFeMnNi high-entropy alloy. *J Alloy Compd.* 2022;922:166259. <https://doi.org/10.1016/j.jallcom.2022.166259>.
  - [48] Wang Q, Kong X, Yu Y, Xin T, Wu L. Effect of B and Hf doping on vacancy defects in AlCrMoNbZr high entropy alloy: a first principles study. *J Phys Chem Solids.* 2024;195:112245. <https://doi.org/10.1016/j.jpcs.2024.112245>.
  - [49] Lukianova OA, Kulitckii V, Rao Z, Li Z, Wilde G, Divinski SV. Self-diffusion in carbon-alloyed CoCrFeMnNi high entropy alloys. *Acta Mater.* 2022;237:118136. <https://doi.org/10.1016/j.actamat.2022.118136>.
  - [50] Cao BX, Wang C, Yang T, Liu CT. Cocktail effects in understanding the stability and properties of face-centered-cubic high-entropy alloys at ambient and cryogenic temperatures. *Scr Mater.* 2020;187:250–5. <https://doi.org/10.1016/j.scriptamat.2020.06.008>.
  - [51] Sun X, Lu S, Xie R, An X, Li W, Zhang T, Liang C, Ding X, Wang Y, Zhang H, Vitos L. Can experiment determine the stacking fault energy of metastable alloys? *Mater Des.* 2021;199:109396. <https://doi.org/10.1016/j.matdes.2020.109396>.
  - [52] Li H, Han Y, Feng H, Zhou G, Jiang Z, Cai M, Li Y, Huang M. Enhanced strength-ductility synergy via high dislocation density-induced strain hardening in nitrogen interstitial CrMnFeCoNi high-entropy alloy. *J Mater Sci Technol.* 2023;141:184–92. <https://doi.org/10.1016/j.jmst.2022.09.020>.
  - [53] Fu Z, Yang B, Gan K, Yan D, Li Z, Gou G, Chen H, Wang Z. Improving the hydrogen embrittlement resistance of a selective laser melted high-entropy alloy via modifying the cellular structures. *Corros Sci.* 2021;190:109695. <https://doi.org/10.1016/j.corsci.2021.109695>.
  - [54] Luo H, Li Z, Raabe D. Hydrogen enhances strength and ductility of an equiatomic high-entropy alloy. *Sci Rep.* 2017;7(1):9892. <https://doi.org/10.1038/s41598-017-10774-4>.
  - [55] Semenyuk A, Klimova M, Shaysultanov D, Salishchev G, Zharebtsov S, Stepanov N. Effect of nitrogen on microstructure and mechanical properties of the CoCrFeMnNi high-entropy alloy after cold rolling and subsequent annealing. *J Alloy Compd.* 2021;888:161452. <https://doi.org/10.1016/j.jallcom.2021.161452>.
  - [56] Li Z. Interstitial equiatomic CoCrFeMnNi high-entropy alloys: carbon content, microstructure, and compositional homogeneity effects on deformation behavior. *Acta Mater.* 2019;164:400–12. <https://doi.org/10.1016/j.actamat.2018.10.050>.
  - [57] Chen Y, Ma J, Lin Y, Hora Y, Zhou Z, Slattery A, An X, Xie Z. Interstitial engineering enabling superior mechanical properties of nitrogen-supersaturated Fe<sub>50</sub>Mn<sub>30</sub>Co<sub>10</sub>Cr<sub>10</sub> high-entropy alloys. *Acta Mater.* 2024;277:120214. <https://doi.org/10.1016/j.actamat.2024.120214>.
  - [58] De Cooman BC, Estrin Y, Kim SK. Twinning-induced plasticity (TWIP) steels. *Acta Mater.* 2018;142:283–362. <https://doi.org/10.1016/j.actamat.2017.06.046>.
  - [59] Li Z, Tasan CC, Springer H, Gault B, Raabe D. Interstitial atoms enable joint twinning and transformation induced plasticity in strong and ductile high-entropy alloys. *Sci Rep.* 2017;7:40704. <https://doi.org/10.1038/srep40704>.
  - [60] Guan HQ, Jing YM, Huang SS. Atomic study of hydrogen behaviors at  $\Sigma$ 3(111) grain boundary in equiatomic CoCrNi and CoCrNiFe alloys. *Tungsten.* 2022;4(3):239–47. <https://doi.org/10.1007/s42864-022-00152-7>.
  - [61] Yuan X, Wu Y, Zhou M, Liu X, Wang H, Jiang S, Zhang X, Wu H, Liu X, Chen Z, Xu X, Lu Z. Effects of trace elements on mechanical properties of the TiZrHfNb high-entropy alloy. *J Mater Sci Technol.* 2023;152:135–47. <https://doi.org/10.1016/j.jmst.2022.12.025>.
  - [62] Wang Z, Wu H, Wu Y, Huang H, Zhu X, Zhang Y, Zhu H, Yuan X, Chen Q, Wang S, Liu X, Wang H, Jiang S, Kim MJ, Lu Z. Solving oxygen embrittlement of refractory high-entropy alloy via grain boundary engineering. *Material Today.* 2022;54:83–9. <https://doi.org/10.1016/j.mattod.2022.02.006>.
  - [63] Baker I. Interstitial strengthening in f.c.c. metals and alloys. *Adv Powder Mater.* 2022;1(4):100034. <https://doi.org/10.1016/j.apmate.2022.100034>.
  - [64] Gan K, Yan D, Zhu S, Li Z. Interstitial effects on the incipient plasticity and dislocation behavior of a metastable high-entropy alloy: nanoindentation experiments and statistical modeling. *Acta Mater.* 2021;206:116633. <https://doi.org/10.1016/j.actamat.2021.116633>.
  - [65] Kim DH, Moallemi M, Kim KS, Kim SJ. Hydrogen embrittlement micromechanisms and direct observations of hydrogen transportation by dislocations during deformation in a carbon-doped medium entropy alloy. *J Mater Res Technol.* 2022;20:18–25. <https://doi.org/10.1016/j.jmrt.2022.07.061>.
  - [66] Yang T, Zhao YL, Li WP, Yu CY, Luan JH, Lin DY, Fan L, Jiao ZB, Liu WH, Liu XJ, Kai JJ, Huang JC, Liu CT. Ultra-high-strength and ductile superlattice alloys with nanoscale disordered interfaces. *Science.* 2020;369(6502):427. <https://doi.org/10.1126/science.abb6830>.